The North African Journal of Scientific Publishing (NAJSP)
مجلة شمال إفريقيا للنشر العلمي (NAJSP)
E-ISSN: 2959-4820
Volume 4, Issue 3, 2026
Page No: 136-152
Website: https://najsp.com/index.php/home/index
SJIFactor 2024: 5.49 | معامل التأثير العربي (AIF) 2025: 0.69 | ISI 2024: 0.696

Studying of CFRP Position for Strengthened Continuous RC T-Section Beams in Negative Moment Zone

Rahma F. Hasson*
Civil Engineering Department, Sirte University, Sirte, Libya.

دراسة موضع صفائح البوليمر المقوى بألياف الكربون *(CFRP)* لتقوية الكمرات الخرسانية المسلحة المستمرة ذات المقطع *T* في منطقة العزم السالب

رحمة ف. حسون*
قسم الهندسة المدنية، جامعة سرت، ليبيا

*Corresponding author: rahma.faraj@su.edu.ly

Received: April 27, 2026	Accepted: July 05, 2026	Published: July 19, 2026

Abstract:
Although carbon fiber reinforced polymer (CFRP) laminates are used widely either for repairing or strengthening of many structures, no enough information is available when used for strengthening of RC continuous T-section beams is available. This is more obvious when used for strengthening of the negative moment zone at the intermediate supports. Moreover, no literature is available for the studying of the expected locations of the laminates across the width of the beam flange which is very important from a practical point of view. Although, it is traditional to consider CFRP laminates fixed above the beam web, this is not practical since walls and columns are located in such locations as a general. This paper examines the effect of varying the locations of CFRP laminates used for the strengthening of the negative moment zone across the beam flange. The Finite Element (FE) Package ANSYS is used to create 3-D theoretical models of this study. From the results of this study, it can be concluded that changing the location of CFRP in the negative moment zone, is important and affects the overall behavior. The optimal locations are either above the web or at the flange adjacent to the web.

Keywords: CFRP, continuous, beam, RC, strengthening, negative moment, T-section, location, ANSYS.

الملخص:
على الرغم من الاستخدام الواسع لصفائح البوليمر المقوى بألياف الكربون (CFRP) في إصلاح وتقوية العديد من المنشآت، إلا أن المعلومات المتاحة حول استخدامها في تقوية الكمرات الخرسانية المسلحة المستمرة ذات المقطع على شكل T لا تزال محدودة، ويظهر هذا النقص بشكل أوضح عند استخدامها لتقوية منطقة العزم السالب عند المساند الداخلية. إضافة إلى ذلك، لا تتوفر دراسات كافية تتناول المواقع المتوقعة لتثبيت الصفائح عبر عرض جناح الكمرة، وهو جانب ذو أهمية كبيرة من الناحية العملية. وعلى الرغم من أن الممارسة التقليدية تفترض تثبيت صفائح CFRP فوق جسم الكمرة (Web)، فإن هذا الحل قد لا يكون عملياً في كثير من الحالات نظراً لوجود الجدران أو الأعمدة في هذه المواضع .تهدف هذه الدراسة إلى فحص تأثير تغيير مواقع صفائح CFRP المستخدمة في تقوية منطقة العزم السالب عبر عرض جناح الكمرة. تم استخدام برنامج العناصر المحددة ANSYS لإنشاء نماذج نظرية ثلاثية الأبعاد لهذه الدراسة .وأظهرت النتائج

أن تغيير موقع صفائح CFRP في منطقة العزم السالب له تأثير ملحوظ على السلوك العام للكمرة، كما تبين أن المواقع المثلى لتثبيت الصفائح تكون إما فوق الجسم مباشرة أو عند الجناح بالقرب من الجسم.

الكلمات المفتاحية: بوليمر مسلح بألياف الكربون (CFRP)، عتبة مستمرة، خرسانة مسلحة، تدعيم، عزم سالب، مقطع T، موقع، برنامج ANSYS.

Introduction:

Only little literature is available considering the behavior of two-span continuous beams with rectangular sections strengthened using CFRP laminates. Experimentally, an external strengthening using CFRP laminates was found to increase the load capacity of such beams. Also, moment redistribution in continuous beams is possible if the longitudinal and transverse reinforcement configuration is chosen properly [1]. Increasing the number of CFRP layers, not beyond its optimum value, increases the flexural capacity. However, it decreases ductility, moment redistribution, and ultimate strain on CFRP laminates [2,3,4].

Extending the CFRP length to cover the entire negative or positive zones did not prevent peeling failure of the CFRP laminates [3]. It has been demonstrated that the deboning mechanisms are influenced by shear forces and moment redistribution that take place in multi-span beams [5]. In addition to increasing the thickness of CFRP laminates and strengthening both the negative and positive regions, end anchorage techniques significantly enhance the response of reinforced high-strength concrete (RHSC) continuous beams [2]. It was shown that externally strengthened RC beams with bonded CFRP laminates have significant increases in their ultimate loads [6]. CFRP strengthening restricts the rotation of plastic hinges at their locations, allowing the formation of additional plastic hinges in unstrengthened cross-sections [5].

On the other side-se T-section beams are highly important as they consider the interaction between beams and slabs. However, very rare research is available about T-section simple or continuous beams strengthened using CFRP laminates. M. M. Rahman et al [7] presented an effective technique of applying CFRP laminate for strengthening the negative zone of continuous T beam considering column constrains. It was found [8] The study explores the history, properties, and research trends of FRP composites, evaluates various strengthening techniques using FRP, and discusses the accuracy of finite element modeling in predicting performance [9]. The use of CFRP splay anchors to secure CFRP laminates had a positive impact on the flexural capacity of the specimens. This anchorage enhanced the load-carrying capacity by 60–104% compared to the strengthened control specimen and by 14–28% relative to the strengthened specimen without anchorage. Criteria to determine the optimum length of CFRP laminate was conducted. However, the optimum length of CFRP laminate should change with the change of the upper reinforcement. The object of this paper is to study the effect of the locations of CFRP laminates across the flange of T-section continuous beams in the negative moment zone.

FE Modeling:

Finite Element modeling is a very effective alternative to the experimental work which is cost and affected by the human mistakes. In order to verify the proposed FE model, the results of an experimental model and well-known theoretical model were compared to those of the proposed model.

Details of Finite Element Modeling: In the following sections, a brief for the process of FE modeling used in this study is explained.

Element Types:

Five types of elements; are used for 3-D modeling of the tested beams, as follows:

- SOLID65 is characterized by eight nodes, each having three degrees of freedom: translations in the x, y, and z directions at each node. The solid is capable of experiencing cracking under tension and crushing under compression. It is used for the modeling of concrete elements.
- LINK180 is a uniaxial tension-compression element with three degrees of freedom at each node, corresponding to translations along the x, y, and z axes. It is used for the modeling of steel reinforcement bars and stirrups.
- SHELL181 is a 4-node element with six degrees of freedom at each node: translations in the x, y, and z directions, and rotations about the x, y, and z-axes. As it may be used for layered applications for modeling laminated composite, it is used for the modeling of CFRP laminates.
- CONTA173 is a 3-D contact element that is used to represent contact and sliding between “target” surface and a deformable contact surface.
- TARGE170 is a 3-D target element that is used to represent 3-D “target” surfaces for the associated contact elements (CONTA173).
- The target surface refers to the concrete beam surface, while the deformable contact surface is the surface of the CFRP laminates. Both contact and target elements form what is called “Contact Pair”.

- The type of contact pair used is "initially bonded," allowing for sliding, gap, or both between the two surfaces. Also, elements have plasticity, large deformations, and large strain capabilities.

Material properties:

Concrete: The stress-strain curve of concrete was modeled using Thorenfeldt's equations.et. al (1987) [6]. These equations are mainly functioning in the value of the compression strength of concrete (f_c'). Figure (1) shows a typical RC stress-strain curve. Additional concrete material data related to the SOLID65 element must be provided, including shear transfer coefficients and tensile stresses. The shear transfer coefficients range from 0.0, representing a smooth crack with complete loss of shear transfer, to 1.0, representing a rough crack with no shear transfer loss. These coefficients can be specified for both open and closed cracks. Open-crack and close-crack shear coefficients are taken as 0.1 and 0.9, respectively. Ultimate tensile strength f_t is taken as 10% of the compression strength. When the element is cracked or crushed, a small amount of stiffness is added to the element for numerical stability. However, the crushing capability was disabled to ensure model convergence. Additionally, the secant modulus of elasticity was used in the finite element modeling instead of the initial modulus. Finally, Poisson's ratio is taken as 0.2.

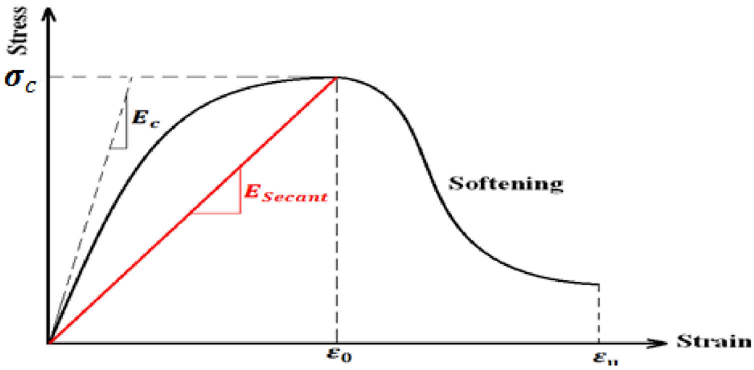

Figure (1): Typical RC Stress-Strain Curve [6].

- **Steel:** Bilinear isotropic hardening material is used to represent the stress-strain curve of steel bars. Required data are modulus of elasticity($E_s = 200{,}000\ MPa$), poisson's ratio($\nu_s = 0.3$), and yield stress ($F_y\ = 400M\ pa$).
- **CFRP:** Multilinear isotropic hardening material is used to represent the stress-strain curve of CFRP laminates shown in Figure (2). The behavior is linear till its maximum stress and then dropped to zero stress at maximum strain.

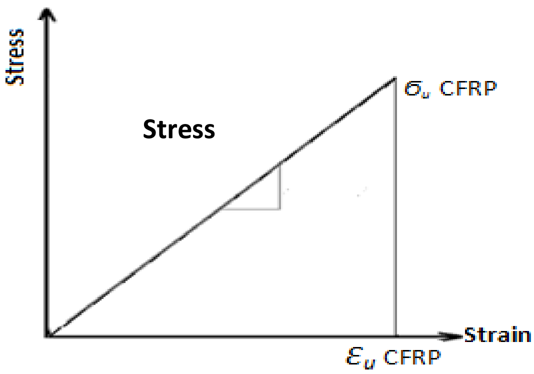

Figure (2): Typical CFRP Stress-Strain Curve.

- **FRP-Concrete Interface (Adhesive):** is modeled using a cohesive zone model (CZM) based on tractions and critical fracture energies to provide debonding properties. This failure criterion takes into account six key parameters: the maximum normal contact stress, critical fracture energy for normal separation, maximum equivalent tangential contact stress, and critical fracture energy for tangential slip, artificial damping coefficient, and flag for tangential slip under compressive normal contact stress. Since Debonding results from shear failure, and the first two parameters were not taken into account. The other four parameters are 6.27 N/mm2, 0.75 N/mm, 0.1, and 1, according to an experimental bond-slip curve by Lu et al. [8]. as shown in Figure (3).

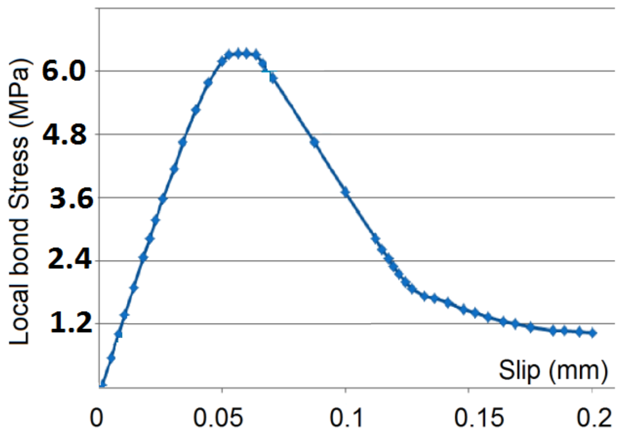

Figure (3): Bond-Slip Curve for Epoxy [8].

Meshing:

A meshing analysis was conducted to determine the optimal solid element size that ensures accurate results with minimal solution time.

Boundary Conditions:

Boundary conditions must suit these of the experimental work and have to take symmetry into consideration, if any, for time saving.

Experimental Model for Verification:

As a part of the experimental program made by M. A. Aiello and L. Ombres [8], the results of beam (S2-0), shown in Figure (4), are used for the verification. In this beam, two CFRP strips at positive region are used and CFRP U-jacketing is used at equal distances. The concrete had an average compressive strength of 21.1 MPa. The steel reinforcing bars had yield strength of 557.0 MPa and a modulus of elasticity of approximately 210.0 GPa. Finally, the CFRP fabric has tensile strength, elastic modulus, and ultimate tensile strain equal 3430 MPa, 230 GPa, and 1.49%, respectively.

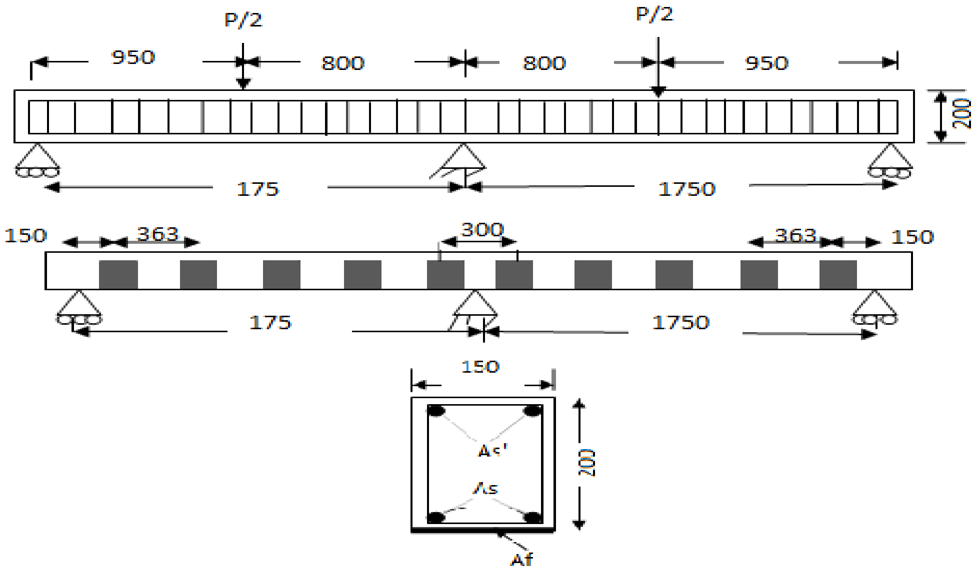

Figure (4): Details of Beam (S2-0).

According to meshing analysis, an element size of: ($x \times y \times z = 50 \times 50 \times 50$ mm) was chosen. The outer two supports were modeled as roller supports to only allow the movement in the direction of the beam axe (direction Z), while the mid-support was pinned support to prevent it from movement in any direction. Due to symmetry, only one quarter of the beam was modeled using the proper boundary conditions at planes of symmetry.

Results for Verification:

Figure (5) shows load versus Mid-Span-deflection of beam (S2-0) due both experimental and FE results. The shown very good agreement insures using ANSYSas a modeling tool for continuous RC beams strengthened by CFRP laminates as follows: Ultimate loads are 205.452 and 201.630 KN due to experimental and finite element results, respectively, with a difference of 1.89%. Maximum deflections are 10 and 10.64mm due to FE and experimental results, respectively, with a difference of -6%.

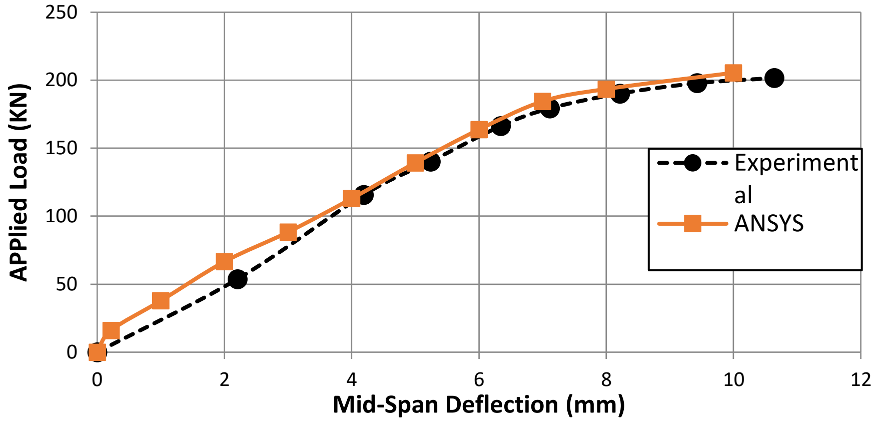

Figure (5): Results of Beam (B2).

Description of the Studied Beams:

A continuous beam with T-cross-section is used for the study, as shown in Figure (6). Each span is subjected to two concentrated loads (P) located at one-third and two-thirds of the span length. By simple statics, as shown in Figure (7), the length of the negative moment zone (LN) equals $(3/4\ L_1)$ or 1500 mm for each of the two spans. The beam was designed using the Egyptian Code of Practice ECP-203 (2007).

The Egyptian Code ECP-208 (2005) was used to obtain the suitable thickness of the CFRP laminates which was 0.9 mm. However, the designed upper reinforcement was reduced by 75% from (4-bars ∯ 24mm) to (4-bars ∯ 12mm) to investigate the effect of CFRP strengthening laminates in this zone.The width of the used CFRP laminate is 300 mm while its length per span is $\mathbf{L_c}$= 1200 mm. Table (1) shows the mechanical properties of the used materials; steel concrete, and CFRP.

Table (1): Mechanical Properties of the Used Materials.

Concrete (MPa)		Steel Bras (MPa)			CFRP Laminates (MPa)	
f'_c	f_t	E_c	f_y	E_s	σ_{u-CFRP}	E_{CFRP}
30	3	26000	400	200000	3050	165000

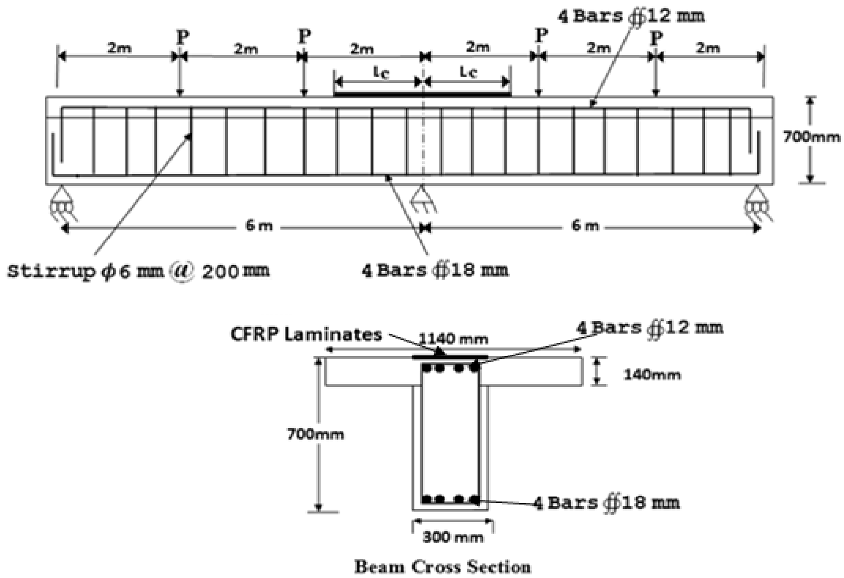

Figure (6): Dimensions and Reinforcement.

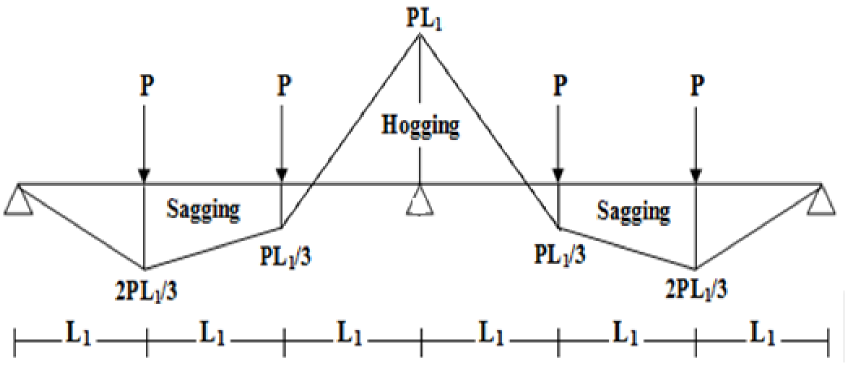

Figure (7): Elastic Bending Moment Diagram.

Effect of the Locations of CFRP Laminates across the Flange:

In this section, different locations across the flange are studied to determine the most suitable and practical location for CFRP laminates. For each location, two lengths for CFRP laminates are used; ($0.80L_N = 1200$ mm), and ($0.40L_N = 600$ mm) to examine if there is an interaction between the location of the laminate and its length. The details are shown in in Figure (8) and Table (2).

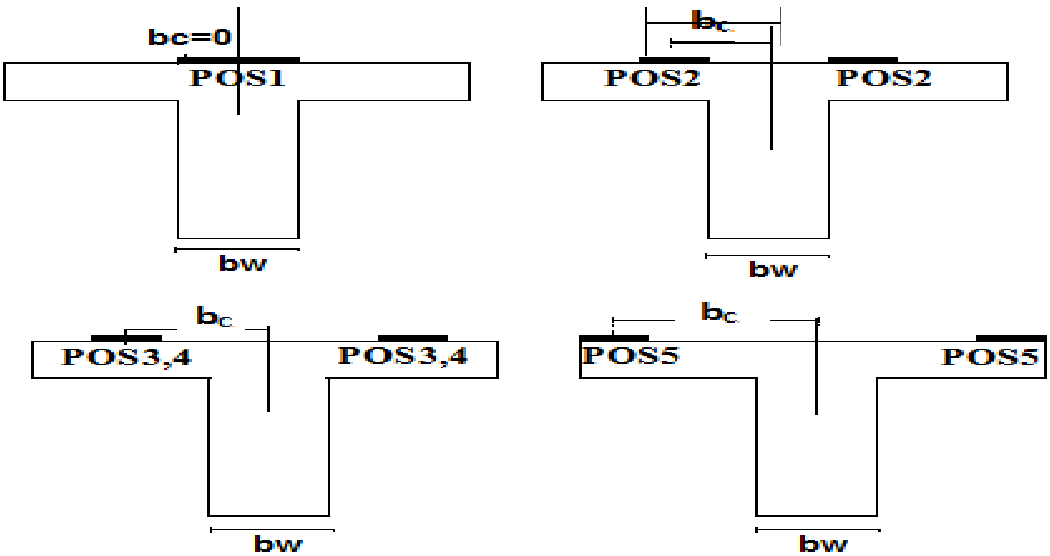

Figure (8): Locations of Laminates across the Flange.

Table (2): Locations of CFRP Laminates.

Location	$\frac{b_C}{b_w}$	0.4L_N (600 mm)	0.8L_N (1200 mm)	Width (CFRP) mm
POS1	0	BS2	BS4	300
POS2	0.75	BS6	BS9	2*(150)
POS3	0.90	BS7	BS10	2*(150)
POS4	1.50	BS8	BS11	2*(150)
POS5	1.65	-----	BS12	2*(150)

Results and Discussions:

Load Deflection Curves:

Figures (9) and (10) show load-deflection curves for the different locations for both lengths 600 and 1200mm, respectively. It is shown that relocating the laminates from web towards flange ends decreases both capacity and deflection of the beam. However, these differences are more obvious in short lengths of CFRP laminates and are generally small.

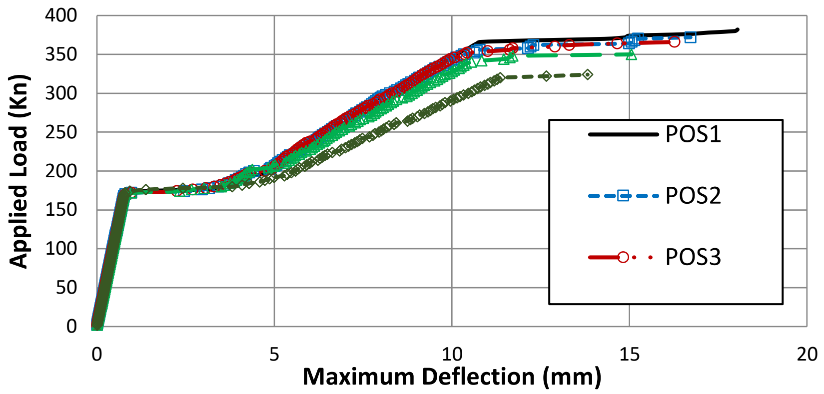

Figure (9): Load – Deflection Curve for ($Lc = 0.40L_N$).

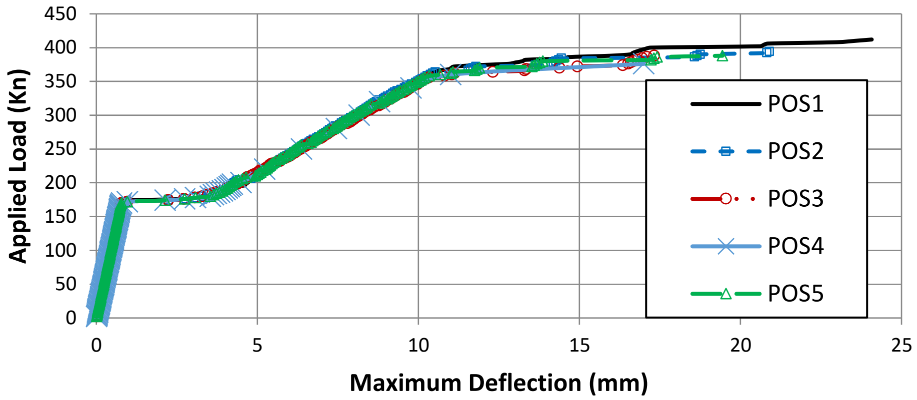

Figure (10): Load –Deflection Curve for ($Lc = 0.80L_N$).

Stresses / Strains of CFRP Laminates at Different Stages of Loadings:

Figures (11), (13), and (15) to (18) show the distribution of stresses in CFRP laminates along their lengths at different stages of loadings for both laminate lengths 600 and 1200 mm. Due to the elastic behavior of the CFRP laminates, strains are distributed in the same manner as stresses as shown in Figures (12), (14), and (19), (20). According to the results, it can be noticed that only at mid-support region, stresses decrease with relocating the laminates from web towards the ends of the flange. After this region, stresses distribution varies along the length of the laminate without certain phenomena; randomly. The worst location is POS4; at the ends of the flange. At this location and as a general, stresses are much less than others which means minimum utilizing of the possibilities of the CFRP laminates. Whatever the location of the strengthening, stresses are gradual. For 1200mm length, the stresses at the ends of the laminates are approximately zero which expresses good transition of stresses without concentration. This is not the case for 600mm length.

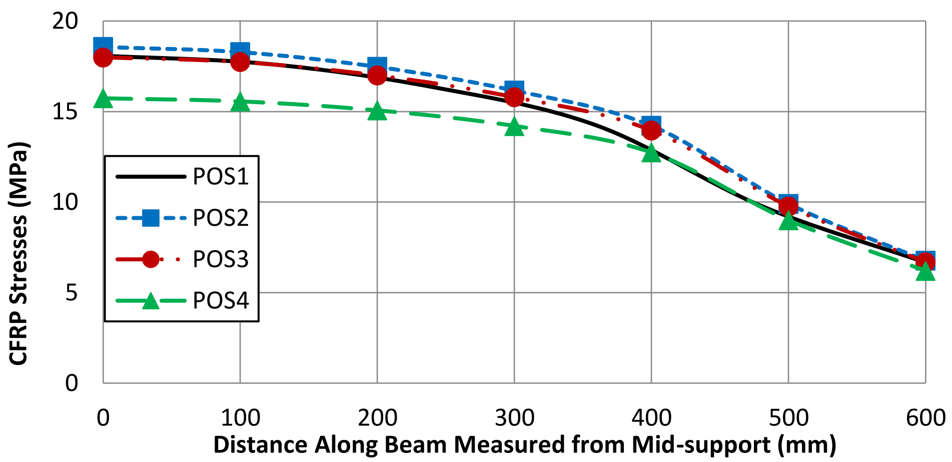

Figure (11): CFRP Stresses at First Crack ($Lc = 0.40L_N$)

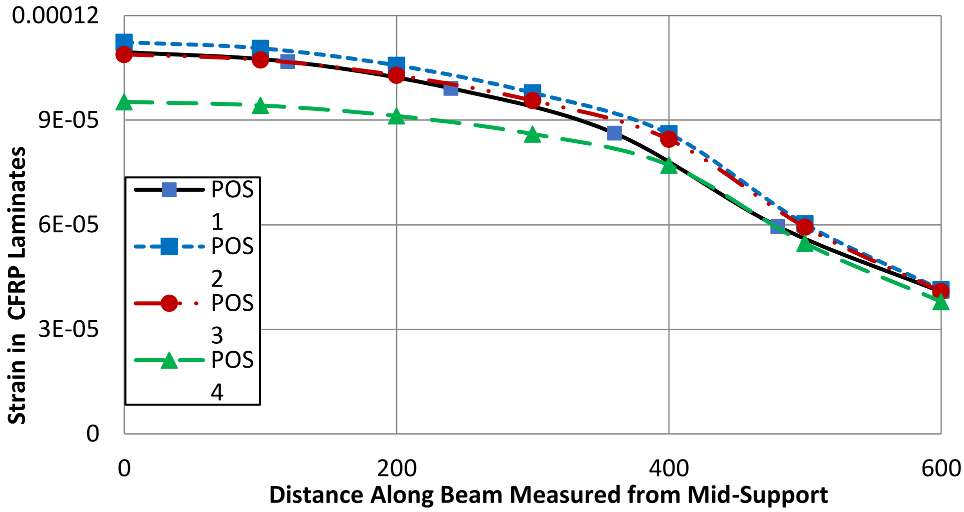

Figure (12): CFRP Strains at First Crack ($Lc = 0.40\mathrm{L_N}$)

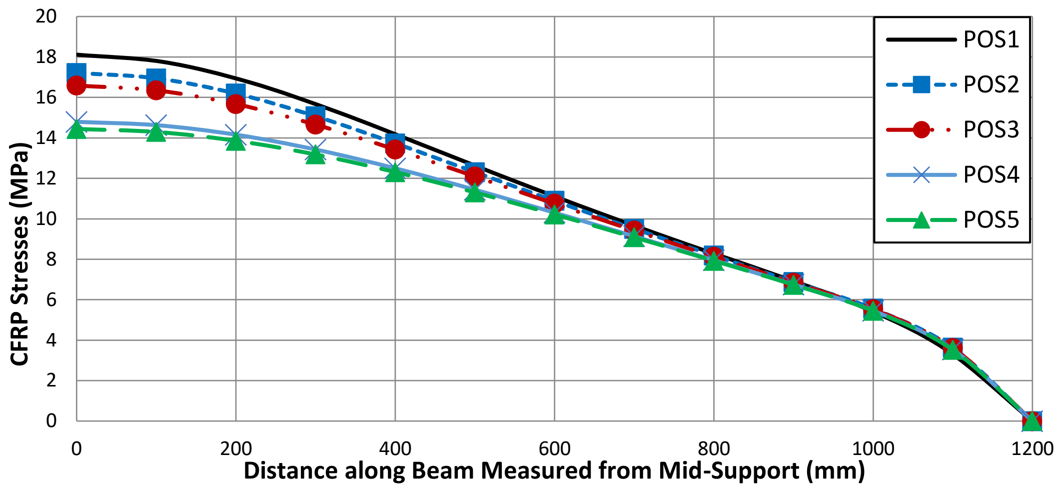

Figure (13): CFRP Stresses at First Crack ($Lc = 0.80\mathrm{L_N}$)

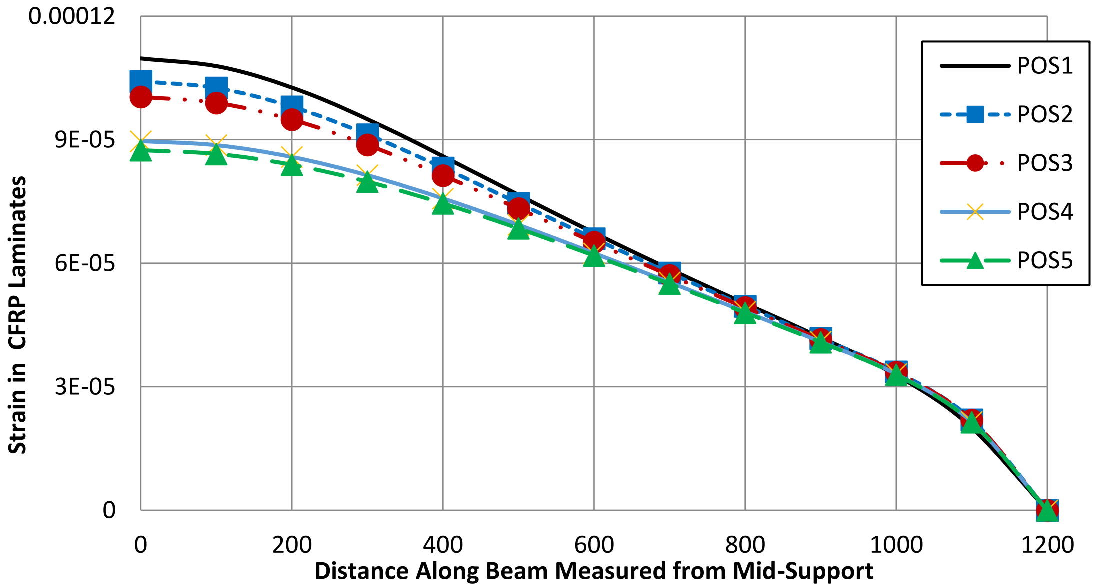

Figure (14): CFRP Strains at First Crack ($Lc = 0.80\mathrm{L_N}$)

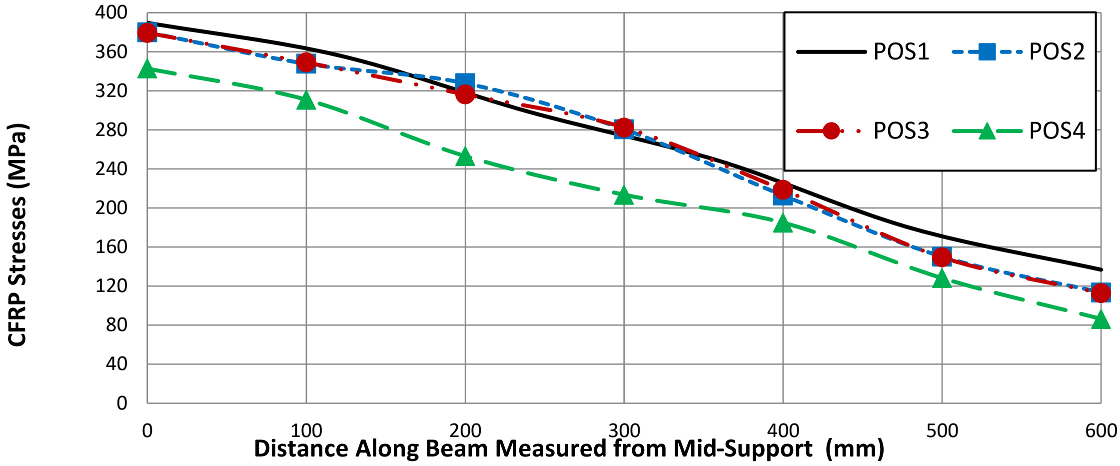

Figure (15): CFRP Stresses at Steel Yield ($Lc = 0.40L_N$)

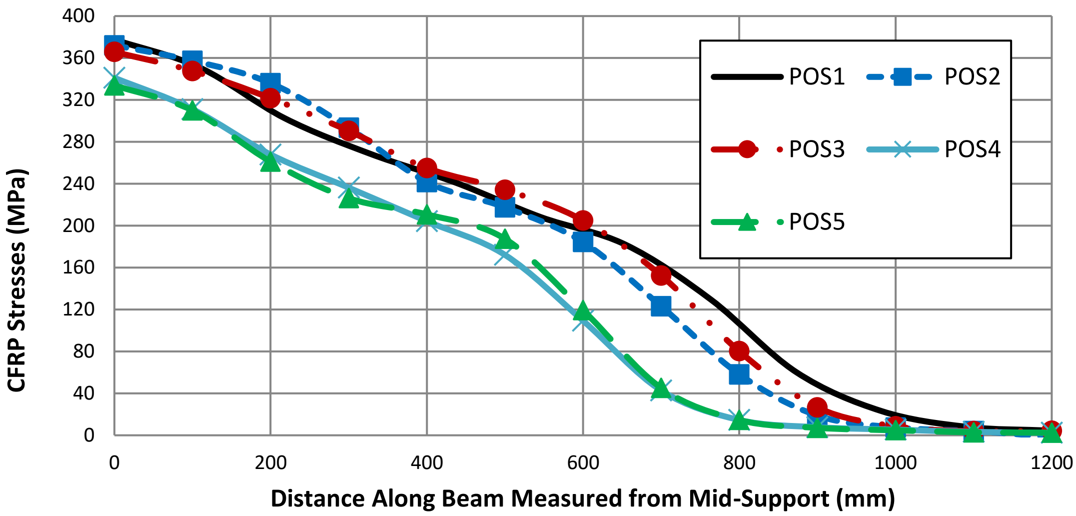

Figure (16): CFRP Stresses at Steel Yield ($Lc = 0.80L_N$)

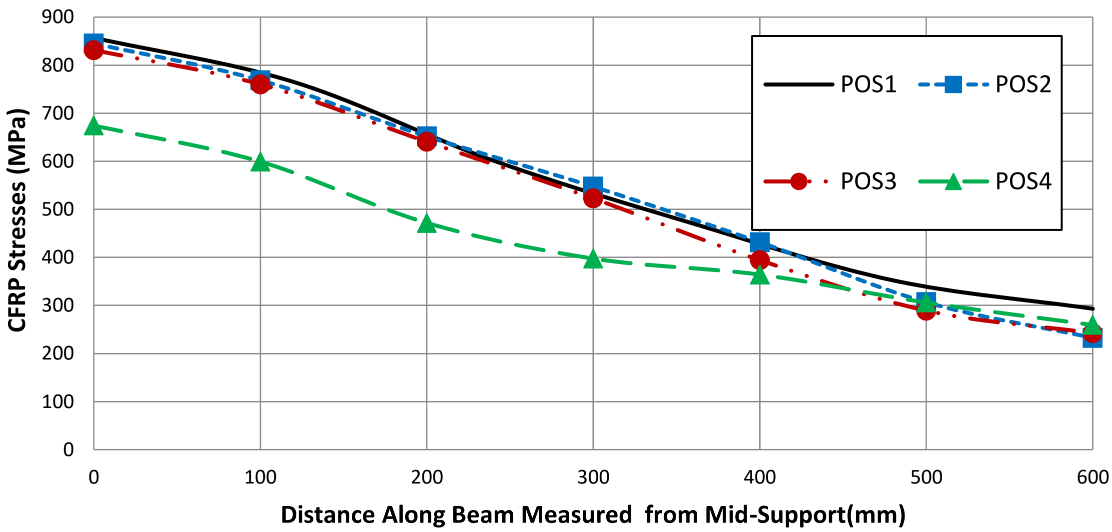

Figure (17): CFRP Stresses at Failure for ($Lc = 0.40L_N$)

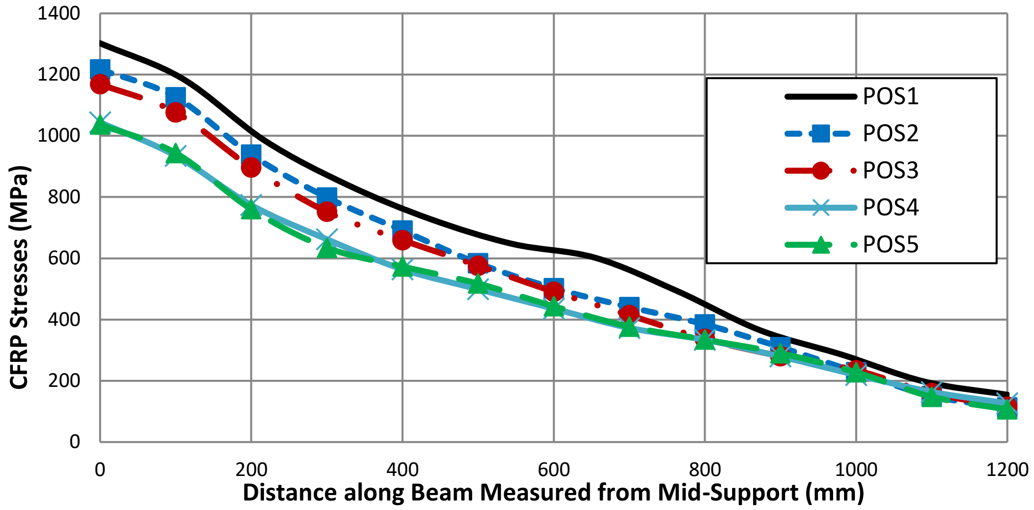

Figure (18): CFRP Stresses at Failure for ($Lc = 0.80L_N$).

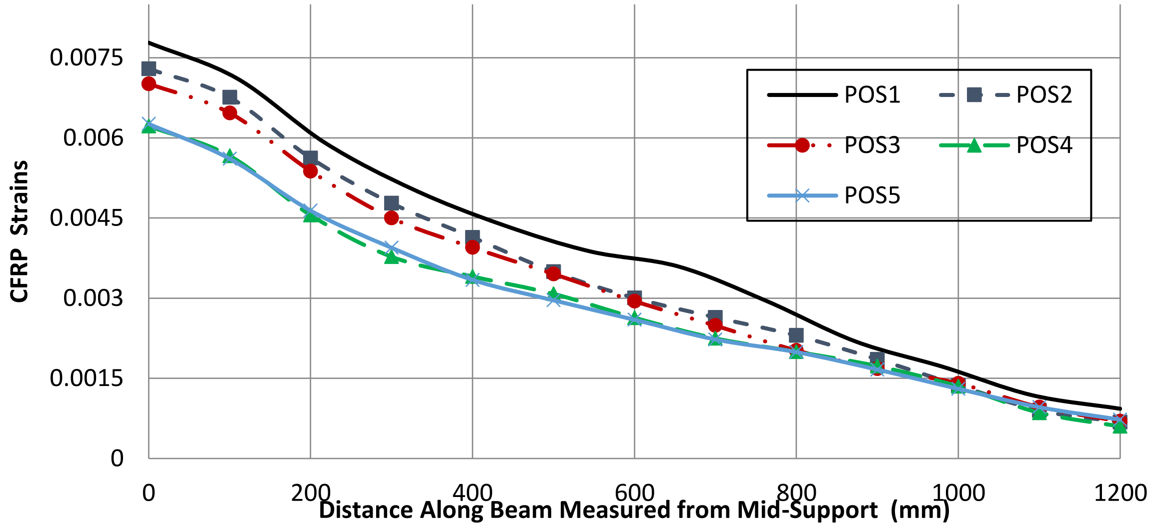

Figure (19): CFRP Strains at Failure for ($Lc = 0.80L_N$).

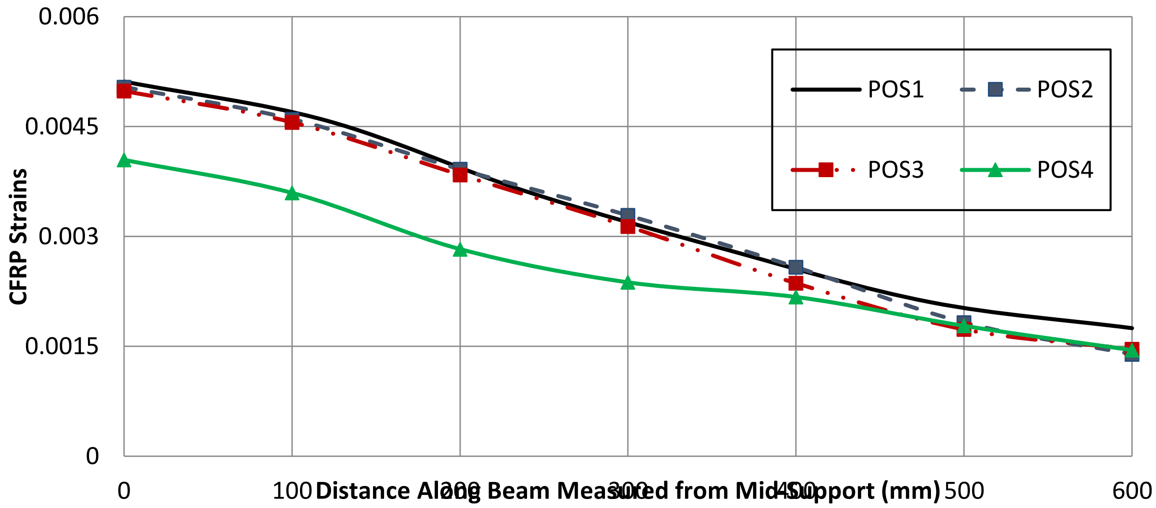

Figure (20): CFRP Strains at Failure for ($Lc = 0.40L_N$).

As a general conclusion, according to [15] and to Figure (18), only about 40% of the capacity of CFRP is reached.

Stresses/Strains of Steel Bars at Different Stages of Loadings:

Figures (21) to (30) show the distribution of stresses and strains of upper steel bars along their lengths at different stages of loadings for lengths 600mm ($\mathrm{L = 0.40L_N}$)and 1200mm ($\mathrm{L = 0.80L_N}$). Until yielding of steel, only stresses are introduced due to the elastic behavior of steel until its yield. According to the results, the following may be obtained:

1. Locations POS1, 2 and 3 can be considered as of the same stress distribution. For POS4 and POS5; at the ends of the flange, stresses are less than other locations. This means less utilizing of steel bars.
2. Strains, at mid-support region, increase with moving away the web. Strains of POS4 and POS5 are about 200% of that for POS1as shown in Figures (23), (24), (27) and (28). This insures that relocating the laminates away the web, especially at the ends of the flange, decreases the utilizing of the upper steel reinforcement.
3. However, locating of the laminates away the web, especially at the ends of the flange, decreases the concentration of strains in steel bars at the end of the short CFRP laminates (600mm length).

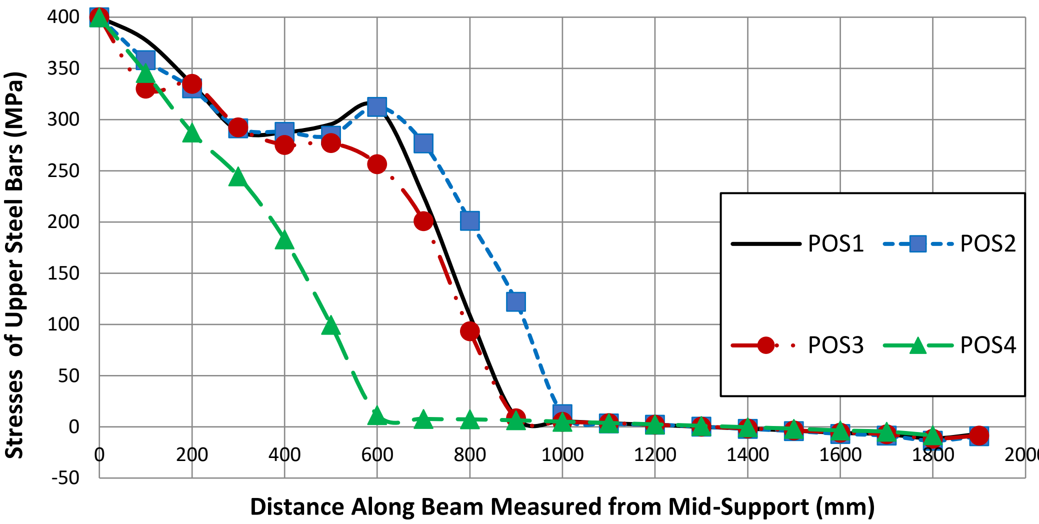

Figure (21): Stresses in Upper Steel Bars at Yielding of Steel for ($\mathrm{Lc = 0.40L_N}$).

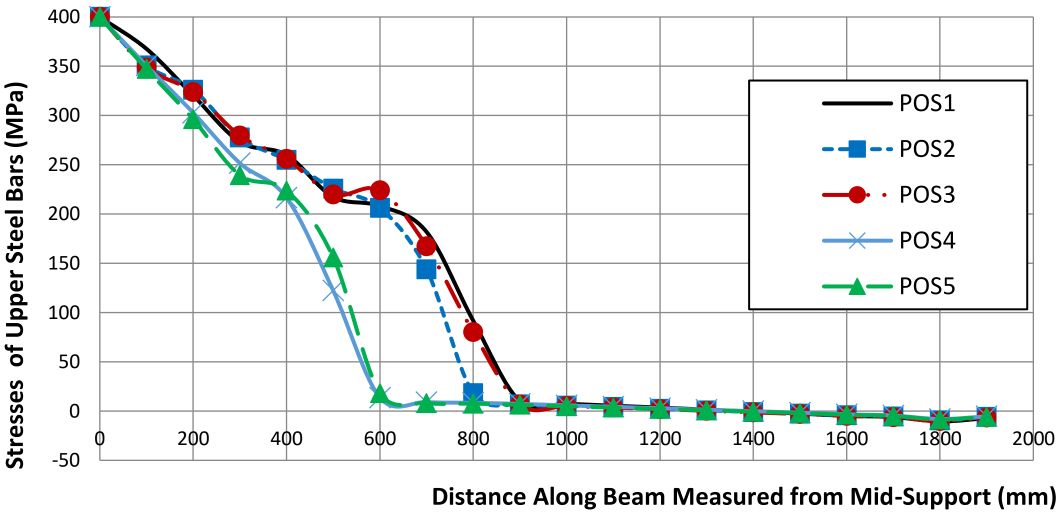

Figure (22): Stresses in Upper Steel Bars at Yielding of Steel for ($\mathrm{L = 0.80L_N}$).

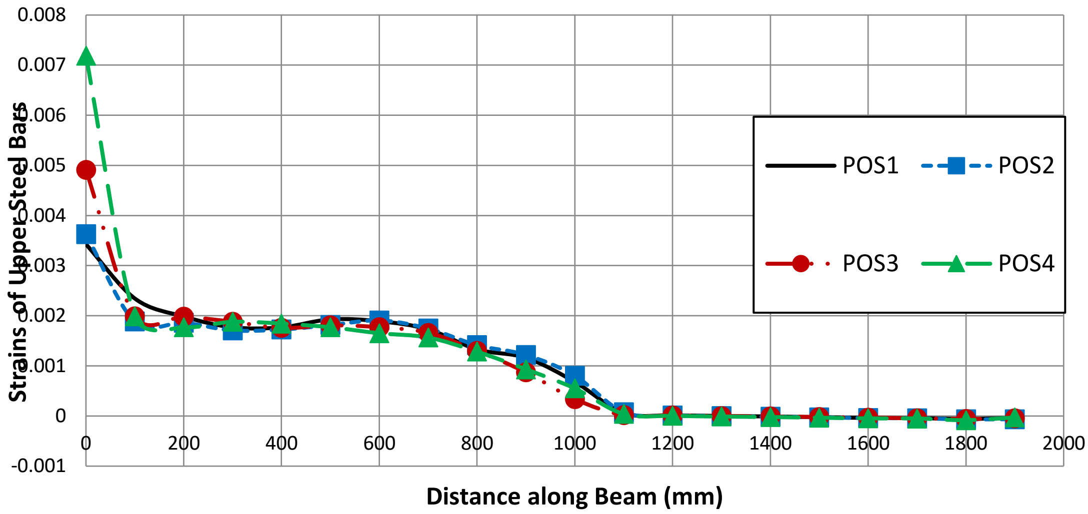

Figure (23): Strains in Upper Steel Bars between Steel Yield and Failure for ($Lc = 0.40L_N$).

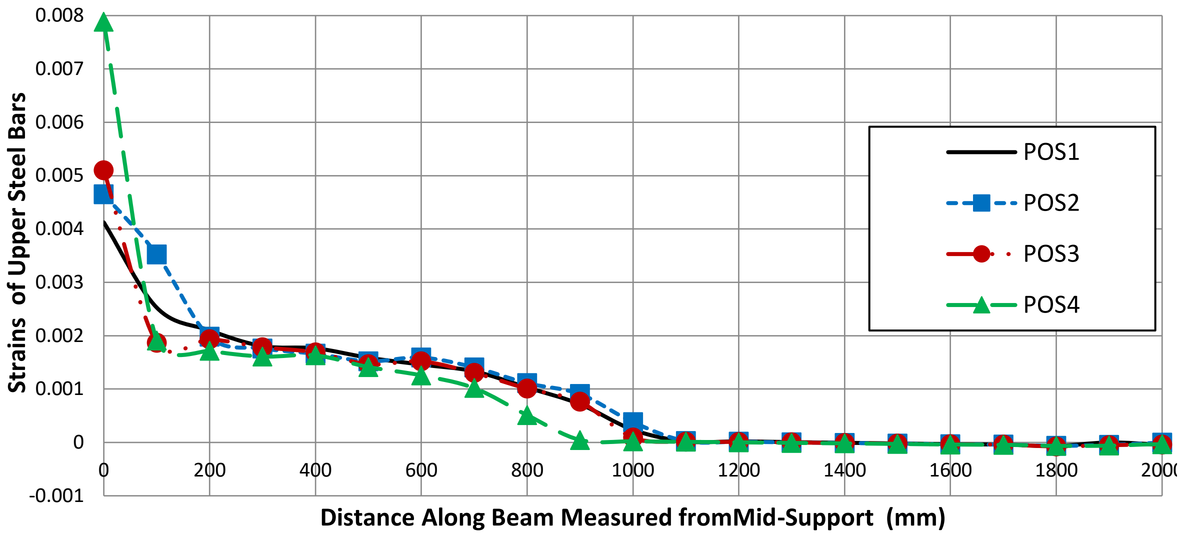

Figure (24): Strains in Upper Steel Bars between Steel Yield and Failure for ($Lc = 0.80L_N$).

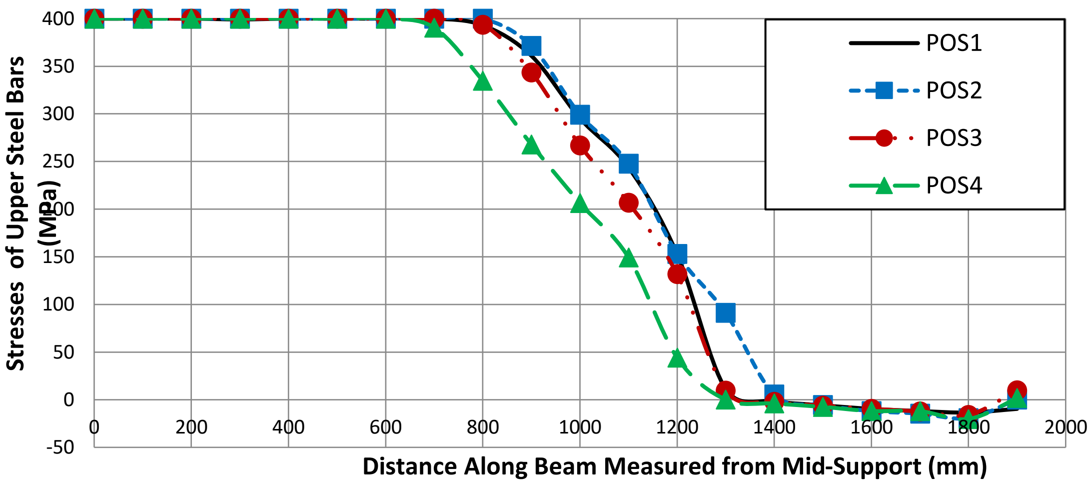

Figure (25): Stresses in Upper Steel Bars at Failure for (Lc $=0.40L_N$).

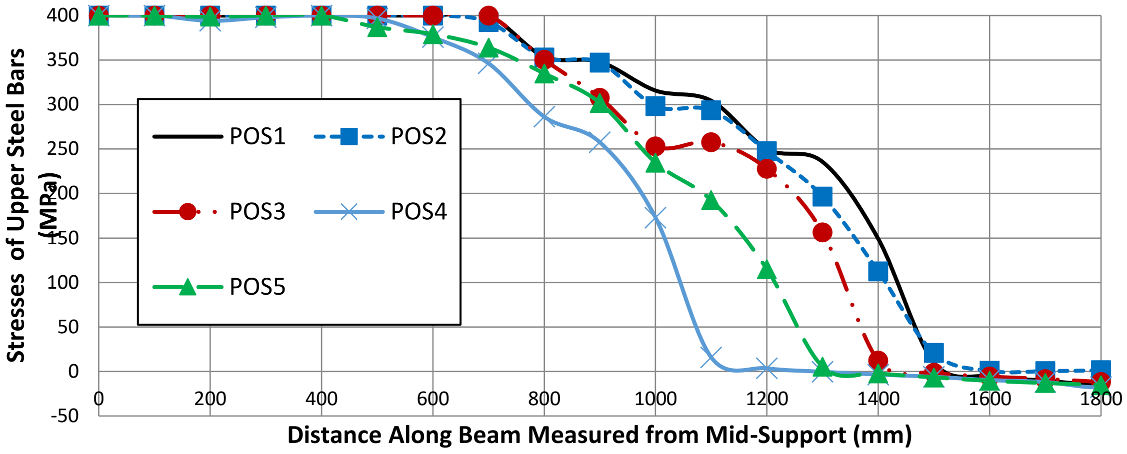

Figure (26): Stresses in Upper Steel Bars at Failure for ($Lc = 0.80L_N$).

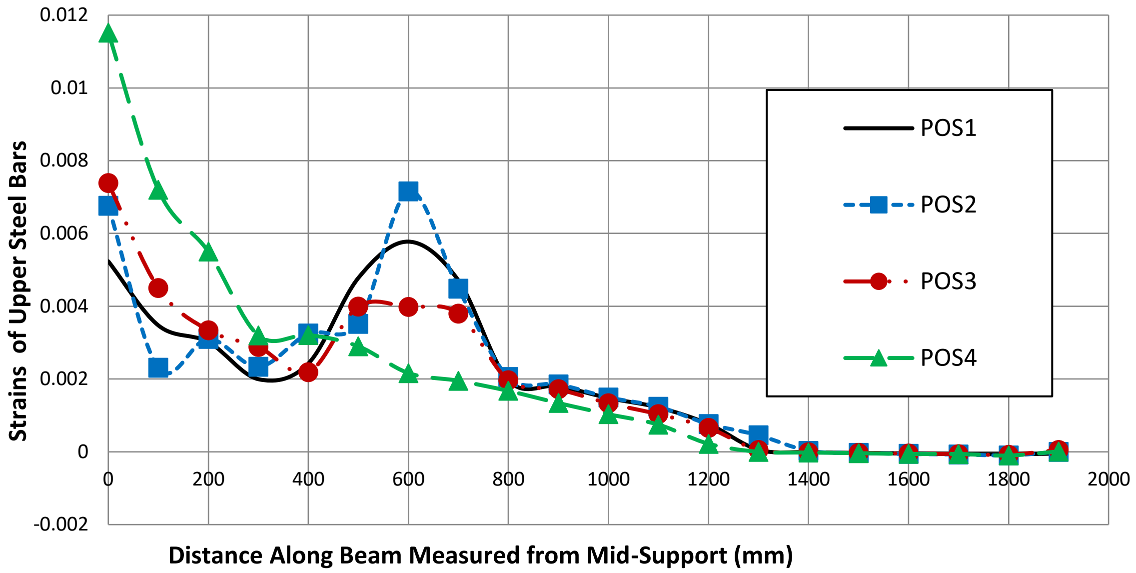

Figure (27): Strains in Upper Steel Bars at Failure for ($Lc = 0.40L_N$).

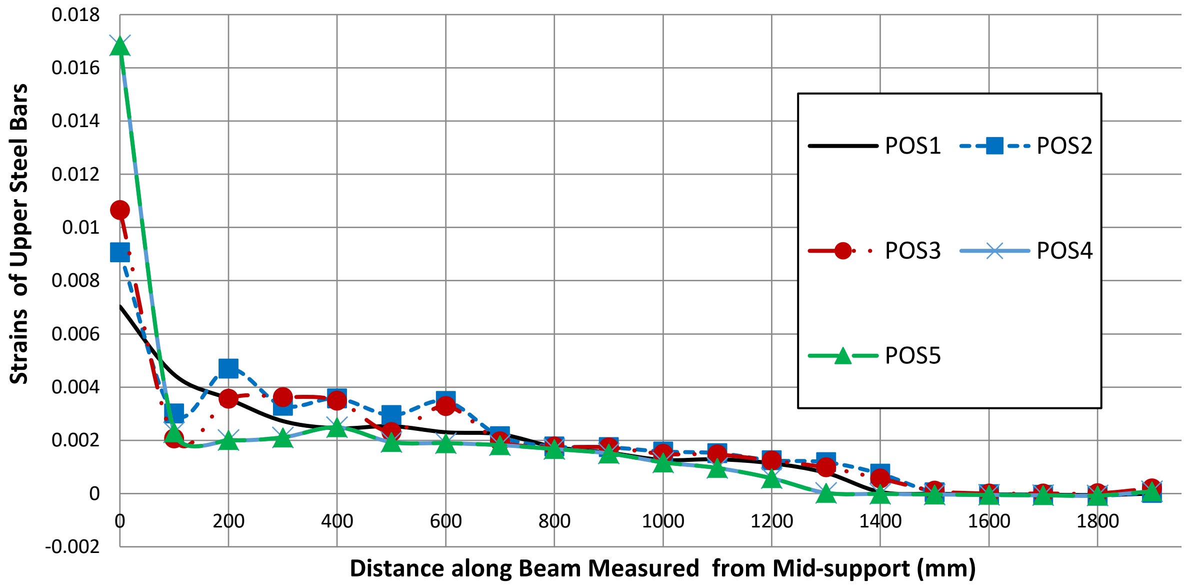

Figure (28): Strains in Upper Steel Bars at Failure for ($Lc = 0.80L_N$).

Assembly of the Previous Results at Failure:

Tables (3) and (4) show the results of the studied FE models at failure. These results are maximum deflection, maximum load, maximum moments either positive or negative, maximum CFRP stresses, and maximum steel strains.

Table (3): Results of Models with CFRP Length of 0.40 HMZ = 600mm, at Failure.

Location	Deflection (mm)	Maximum Load (kN)	Negative Moment (N.mm)	Positive Moment (N.mm)	Maximum Stress of CFRP (MPa)	Maximum Strain of Steel
POS1	382	18	298.62	282.48	856.94	.00523
POS2	372 97.38*	16.7 92.78*	297.00 99.46*	272.00 96.29*	845.18 98.63*	.00676 129.25*
POS3	366 95.81*	16.3 90.55*	286.44 95.92*	270.50 95.76*	831.33 97.01*	.00738 141.11*
POS4	350 91.62*	15.1 83.89*	244.80 81.98*	268.40 95.02*	674.37 78.70*	.0115 219.89*

*Percentage between the value across the flange and this on the web.

Table (4): Results of Models with CFRP Length of 0.80 HMZ = 1200mm, at Failure.

Location	Deflection (mm)	Maximum Load (kN)	Negative Moment (N.mm)	Positive Moment (N.mm)	Maximum Stress of CFRP (MPa)	Maximum Strain of Steel
POS1	412	24.1	378.00	286.00	1302.4	.00703
POS2	394 95.63*	20.9 86.72*	353.00 93.39*	276.12 96.55*	1217 93.44*	.00906 128.88*
POS3	392 95.15*	19.6 81.33*	344.00 91.00*	273.33 95.57*	1168.5 89.72*	.0107 152.20*
POS4	376 91.26*	16.5 68.46*	313.44 82.92*	271.52 94.94*	1037 79.62*	.0168 238.98*
POS5	375 91.02*	16.3 67.63*	312.69 82.72*	270.60 94.62*	1034 79.39*	.0168 238.98*

*Percentage between the value across the flange and this on the web.

Moment Redistribution:

In this section, redistribution of moments between both positive and negative moments is examined. This redistribution allows good utilizing of the beam capacity.

Moment redistribution factor (β) **is defined as:**

$$\beta = \left(\frac{M_{FE}-M_E}{M_E}\right) \times 100 \quad \% \qquad (1)$$

M_{FE} is the bending moment calculated from FE results at failure (using both failure loads and their corresponding reactions), and M_E is the failure bending moment calculated elastically due to failure load. Tables (5) and (6), and Figure (29) show the values of the redistribution ratio (β) for the different locations of CFRP laminates for lengths 600mm ($Lc = 0.40L_N$) and 1200mm ($Lc = 0.80L_N$), respectively.

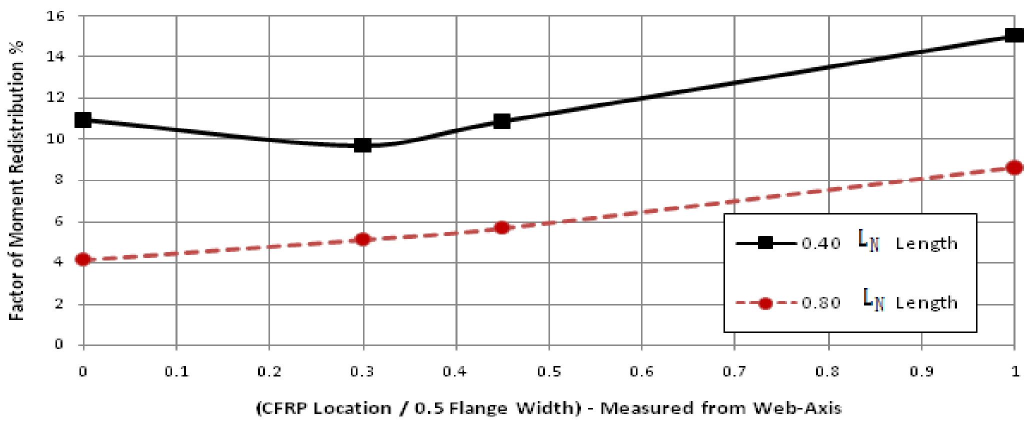

Figure (29): Factor of Moment Redistribution (β) along Beam Flange

According to the previous results:

For long CFRP lengths ($0.80L_N = 1200$ mm), moment redistribution factor (β) increases with relocating of the laminates away from the web. The maximum increasing occurs when CFRP laminate is fixed at the ends of the flange.

For short CFRP lengths ($0.40L_N = 600$ mm), moment redistribution factor (β) is maximum at the ends of the flange. It is much bigger than other three locations. These three locations have close values of the factor (β) without certain order. However, the minimum factor (β) lies at the two beginnings o the flange; just beside the web.

Negative moment (at the central support) decreases with relocating of CFRP laminates away from the web-axis towards the ends of the flange. Table (7) and Figure (30) show the percentage of this decreasing for the different locations related to the location located at the web

Table (5): Values of Moment Redistribution Factor (β) due to Relocating for Length 600mm.

Location of CFRP	Model No.	P_u (kN)	Reactions (kN)		M-ve at Mid-Support			M+ve within Span		
			Mid-Support	End Support	M_{FE} (kN.m)	M_E (kN.m)	β (%)	M_{FE} (kN.m)	M_E (kN.m)	β (%)
POS1	BS2	382	204.77	141.23	298.62	382	-21.83	282.48	254.66	10.92
POS2	BS6	372	235.50	136.50	297.00	372	-20.16	272.00	248.00	9.68
POS3	BS7	366	230.74	135.26	286.44	366	-21.74	270.50	244.00	10.86
POS4	BS8	350	215.80	134.20	244.80	350	-30.06	268.40	233.33	15.03
Control Beeam	CB	326	189.91	136.09	162.00	326	-50.31	272.18	217.00	25.43

Table (6): Values of Moment Redistribution Factor (β) due to Relocating for Length 1200mm.

Location of CFRP	Model No.	P_u (kN)	Reactions (KN)		Mid-Support			Span		
			Mid-Support	End Support	M_{FE} (kN.m)	M_E (kN.m)	β (%)	M_{FE} (kN.m)	M_E (kN.m)	β (%)
POS1	BS4	412	268.98	143.02	378.00	412	-8.25	286.00	274.66	4.13
POS2	BS9	394	255.94	138.06	353.00	394	-10.41	276.12	262.66	5.12
POS3	BS10	388	251.34	136.66	344.00	388	-11.34	273.33	258.66	5.67
POS5	BS12	376	240.24	135.76	313.44	376	-16.64	271.52	250	8.61
Control Beam	CB	326	189.91	136.09	162.00	326	-50.31	272.18	217.00	25.43

Table (7): Percentage of Moment Decreasing Related to the Location Located at the Web.

Location of CFRP	CFRP Length = 0.4 LN = 600 mm			CFRP Length = 0.4 LN = 1200 mm		
	P_u (KN)	M_{FE} (kN.m)	ΔM %	P_u (KN)	M_{FE} (kN.m)	ΔM %
POS1	382	298.62	------	412	378.00	-----
POS2	372	297.00	-0.54	394	353.00	-6.61
POS3	366	286.44	-4.07	388	344.00	-9.00
POS5	350	244.80	-18.02	376	313.44	-17.08

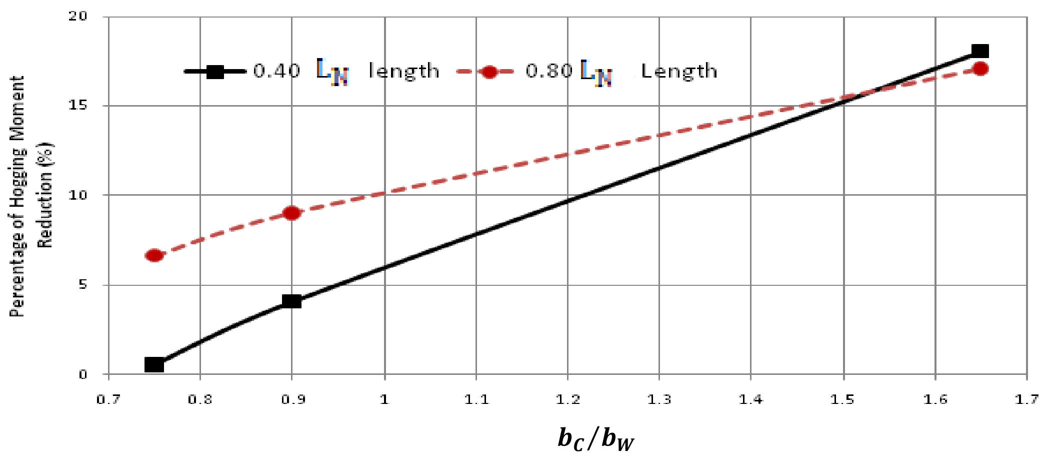

Figure (30): Percentage of Negative Moment Reduction along Beam Flange.

Conclusions:

This paper examines the effect of varying the locations of CFRP laminates used for the strengthening of the negative moment zone across the beam flange. The Finite Element (FE) Package ANSYS is used to create 3-D theoretical models of this study. From the results of this study, it can be concluded that:

1. Stresses in upper steel bars, at the ends of the flange, are less than other positions, especially away from the mid-support region.
2. Strains in upper steel bars increase up to 200% with moving away the web.
3. Only for short CFRP laminates (600mm length), the concentration of strains in upper steel bars decreases with moving away from the web.
4. Moment redistribution factor (β) is maximum at the ends of the flange. It is of a minimum value at the web (POS1) for long CFRP lengths, and at the beginnings of the flange (POS2) for short lengths.
5. Negative moment (at the central support) decreases with repositioning of CFRP laminates away from the web.
6. Putting CFRP laminates above the web gives much more utilizing of the concrete compression strength/strain than other positions.
7. Going away from the web towards end of the flange decreases both concrete stresses and strains which means less utilizing of concrete.
8. The presence of CFRP laminates at the top of the beam in the mid-support zone only affects the concrete stresses / strains at the beam top in the mid-span zone.
9. As a conclusion, position POS1 (at the web) is the optimal location for CFRP strengthening laminates, provided there are no walls above the web, the optimal location is to put the CFRP laminates just after the web at both sides of the wall. These positions utilize perfectly both steel bars and CFRP laminates.

Reference:

1. M. A.Sakr, T. M. Khalifa, and W. N.Mansour, “External Strengthening of RC Continuous Beams Using FRP Plates: Finite Element Model”, Proc. of the Second Intl. Conf. on Advances in Civil, Structural and Mechanical Engineering- CSM 2014, ISBN: 978-1-63248-054-5, pp. 168-174, 2014.
2. A. A. Maghsoudi, H. A. Bengar, “Moment redistribution and ductility of RHSC continuous beams strengthened with CFRP”, Turkish Journal of Engineering and Environmental Sciences, http://journals.tubitak.gov.tr/engineering/issues/muh-09-33-1/muh-33-1-5-0901-6.pdf, Vol. 33, pp. 45-59, 2009.
3. Journal of Civil Engineering Construction Technology, http://www.academicjournals.org/JECET, ISSN 1991-637X, Vol. 4, No. 6, pp. 174-183, June 2013.
4. S. A. El-Refaie, A. F. Ashour, and S. W. Garrity, “Positive and Negative Strengthening of Continuous Reinforced Concrete Beams Using Carbon Fiber-Reinforced Polymer Laminates”, ACI Structural Journal, V. 100, No. 4, pp. 446-453, July-August 2003.
5. L. Taerwe, L. Vasseur, and S. Matthys, “External strengthening of continuous beams with CFRP”, Concrete Repair, Rehabilitation and Retrofitting II, London, ISBN 978-0-415-46850-3, pp. 43-53, 2009.
6. A. R. Saleh, and A. A. H. Barem, “Experimental and Theoretical Analysis for Behavior of R.C. Continuous Beams Strengthened by CFRP Laminates”, Journal of Babylon University (Iraq), Engineering Sciences, Vol. 21, No. 5, pp. 1555-1567, 2013.
7. M. El-Mogy, A. El-Ragaby, and E. El-Salakawy, “Experimental testing and finite element modeling on continuous concrete beams reinforced with fibre reinforced polymer bars and stirrups”, Canadian Journal of Civil Engineering, Vol. 40, No. 11, pp. 1091–1102, November 2013.
8. U. S. Shrestha, "Modified Composite Application to Improve Strength and Ductility of Structural Components", Master of Science Thesis, College of Graduate Studies, The University of Toledo, Ottawa, USA, December 2014.
9. W.M.Iesa,M.B.S. Alferjani,N.Ali, and A.A.AbdulSamad, “Study on Shear Strengthening of RC Continuous Beams with Different CFRP Wrapping Schemes”, International Journal of Integrated Engineering (Issue on Civil and Environmental Engineering),http://penerbit.uthm.edu.my/ojs/index.php/ijie/article/view/207, Vol. 2, No. 2, pp. 35-43, 2010.
10. ANSYS, “ANSYS Help”, Release 15.0, 2013
11. S. A. El-Refaie, A. F. Ashour, and S. W. Garrity, “Positive and Negative Strengthening of Continuous Reinforced Concrete Beams Using Carbon Fiber-Reinforced Polymer Laminates”, ACI Structural Journal, V. 100, No. 4, pp. 446-453, July-August 2003.

12. “ECP-208: Egyptian Code for the Design Principals and Implementation Requirements of Using CFRP in Fields of Construction, Housing and Building Research Center (HBRC), Cairo, Egypt, 2005.
13. E. Thorenfeldt, A. Tomaszewicz, and J. Jensen, “Mechanical Properties of High Strength Concrete and Application to Design,” Proceedings of the Symposium: Utilization of High-Strength Concrete”, Stavanger, Norway, Tapir, Trondheim, pp. 149–159, June 1987.
14. Lu XZ, Ten JG, Ye LP, Jaing JJ. Bond-slip models for FRP sheets/plates bonded to
15. concrete. Eng. Struct 2005;24(5):920–37.
16. M. A. Aiello and L. Ombres, "Moment Redistribution in Continuous Fiber-Reinforced Polymer-strengthened Reinforced Concrete Beams", ACI Structural Journal, pp. 158-166, March-April 2011.
17. M. M. Rahman, andM. W. Rahman, “Simplified method of strengthening RC continuous T beam in the negative zone using carbon fiber reinforced polymer laminate - A numerical investigation”,
18. Ali Jahami and Camille A. Issa "An Updated Review on the Effect of CFRP on Flexural Performance of Reinforced Concrete Beams"International Journal of Concrete Structures and Material, (2024) 18:14
19. Maha Assad,Rami A. Hawileh and Jamal A. Abdalla"Flexural Strengthening of Reinforced Concrete Beams Using CFRP Laminates" Vol 13, Mar 2024, 100443.